REMOTE INVESTIGATION OF COMPOSITIONALLY DISTINCT LITHOLOGIES AT AND AROUND THE CENTRAL PEAKS OF SOME RECENT CRATERS AND THEIR IMPLICATIONS FOR CRATER MODIFICATION PROCESS

Mamta Chauhan[1], Prakash Chauhan[1]* and Henal Bhatt[2]

[1]Indian Institute of Remote Sensing (IIRS), Indian Space Research Organization (ISRO), Dehradun - 248001 INDIA and [2]Department of Geology, M. G. Science Institute, Navrangpura, Ahmedabad, 380009.

*** Dr. Prakash Chauhan**

Director,

Indian Institute of Remote Sensing (IIRS)

Indian Space Research Organization (ISRO),

Department of Space, 4, Kalidas Marg,

Dehradun - 248001 INDIA

Phone: +91-0135-252-4100

E-mail address: prakash4140@gmail.com, prakash@iirs.gov.in

Abstract

Central peaks of lunar complex craters of Copernican period provide best examples to study morphologies of impact melts and exposed subsurface as they are better preserved and less affected by the space weathering. Crater Tycho, present towards SW, nearside of the Moon is one such example of young and fresh complex crater. Present study is high-resolution mineralogical investigation coupled with morphological study of central peaks and floor of crater Tycho and other contemporary craters to understand the nature of occurrence and distribution of compositionally distinct lithologies identified near their central peaks that differ in colour and specific appearance. A detailed high-resolution analysis suggests that the clastic exposures associated with the melts have a mafic composition that have been observed at similar other contemporary craters. They represent the fragmental polymict breccia clasts and their stratigraphic relation with the melts alongwith with their mineralogy suggests them to be representative of subsurface anorthositic gabbro/noritic body. Their occurrence and association with structural features, such as breccias dikes and cooling cracks suggest their formation at different stages of cratering and associated crustal modification. The formation mechanism of the polymict breccia clasts causing lithological variability has been discussed. We also report here the occurrence of rejuvenated dykes peculiar to Tycho setting that are distinct from the fractures in the immediate viscinity. Their unique nature suggests different emplacement mechanism associated with dynamic cratering process till not reported at any young complex crater on the Moon.

Keywords-Complex crater, Impact-melts, Cooling cracks, Breccia dyke.

Key Points:

The purposes of this paper is to:

1) Investigate the compositional variability associated with central peaks & floor of Tycho and check for similarity at other contemporary complex craters.
2) To present new findings concerning the modes of occurrence of fragmental polymict breccia clasts over the crater floor
3) To assess the implications for the processes responsible for the modification of the crater after its formation.

Summary:

Crater modification is least understood process, especially the emplacement style of impact melt and fragmental breccia and their relationship with rock deformation. It needs further interpretation of the associated deformation features. The present study attempts to understand the lithological variability occurring at and near the central peak of some recent Copernican age complex craters on the Moon. An attempt have been made to investigate the lithological variability occurring in these young craters and understand the phenomenon which is more prominently displayed at crater Tycho. It has been observed through high-resolution remote sensing and studied in detail. The distribution of mafic highland lithology, their tectonic position and association with structural features, such as breccias dikes and cooling cracks suggest their formation from the deep-seated target that are exposed at different stages of cratering.

1. Introduction

Impact craters' study started relatively late during last few decades of the twentieth century. Various methods based analysis of terrestrial impact craters including geophysical, geochemical, numerical and experimental simulation and hydrocode modeling have added significant understanding of the phenomenon. But not all of its processes are well understood, especially in terms of modification and post modification events (Masaitis, 2005). Limitation arise in our understanding as Earth is geologically active and impact craters being surface features, most of the preserved craters has retained the poorest record throughout the geologic

time. The Moon can serve as an ideal natural laboratory for studying crater morphology and morphometry due to its low gravity, lack of atmosphere that result in higher cratering efficiency than on the other terrestrial planets (Pike 1976; Stoffler et al., 2006). Moon therefore, provides a good opportunity to study these features.

Young complex craters belonging to Copernican age, in particular are the most suitable geological landforms that contribute significantly to understand the cratering phenomenon and its various aspects. These craters being less affected by space weathering effects offers better preserved morphological features for understanding the phenomemon of cratering. Generation as well as emplacement of impact melts and ejected debris formed subsequent to cratering is one of the primary characteristics of these craters. They represent the target subsurface rocks that are uplifted after being hit by high-velocity collider and have occupied the present position after excavation (e.g., Melosh, 1989). The compositional characteristics observed at the complex craters are important in understanding the sub-surface lithology of the planets (Hiesinger & Head, 2006). In addition, they can also provide insight into understanding the various aspects related with modification and post modification stage, especially those associated with the nature and mechanism of emplacement of its various products and related structures.

Crater Tycho (43.4°S, 11.0°W) is one such complex crater, present near to the south-east edge of Oceanus Procellarum. It is the most prominent rayed crater on the Moon having a diameter of about 85 km. This relatively young Copernican aged crater (Stöffler & Ryder 2001; Heisinger et al., 2010) have been studied by various researchers using various remote sensing data (e.g., Hawke & Head, 1977; Hawke & Bell, 1981; Bray et al., 2010; Chauhan et al., 2012, Carter et al., 2012; Dhingra et al., 2017). High-resolution LRO-NAC and Mini-RF observations confirmed the presence of melts flow and ponds associated with embedded clasts from floor of the crater Tycho (Bray et al., 2010; Carter et al., 2012). Mineralogical analysis using Chandrayaan-1 M^3 data, have detected high-Ca pyroxenes (HCP), spinel, crystalline plagioclase and olivine from the central peak as well its crater margin (Ohtake et al., 2009; Chauhan et al., 2012; Kaur et al., 2012). The present study deals with compositional as well as morphological investigation of the floor and central peak of the crater Tycho to throw light over the impact related process that modified the target crust and redistributed it over the surface in various forms and their emplacement behaviour. In order to better understand the observed lithological variability and its emplacement nature some other contemporary craters have been selected to

check for the similarity and comparision. It yet adds a new perspective in understanding the phenomenon especially, the associated various phases related with the modification and post modification stages as observed through high-resolution multiple datasets**.**

2. Methods and Observations

Observations related with composition and topographical variations were investigated using data from ISRO's Chandrayaan-1 Moon Mineralogy Mapper (M^3) and JAXA's Kaguya mission. Visible data of Multiband Imager (MI-VIS) obtained from Kaguya's SELENE (SELenological and ENgineering Explore) having spatial resolution 20 m/px at the nominal altitude (100 km) (Haruyama et al., 2008; Kato et al., 2008) provided the compositions of observed geologic units. Photometrically and thermally corrected reflectance data (Level 2 products) from hyperspectral sensor, Moon Mineralogy Mapper (M^3) of ISRO's Chandrayaan-1 mission have been used for spectral analysis. Its spatial resolution of ~140 m/pixel from 100-km and ~280 m/pixel from 200-km orbits with a wide spectral range of ~0.5-3 μm in 85 spectral channels (Boardman et al. 2011) enabled better evaluation of the mafic mineral constituents.

For understanding topographic variations over the central peak of crater Tycho, Terrain Camera (TC) of SELENE with spatial resolution of 10 m/px has been used. To characterize the three-dimensional configuration of the impact melt flow features and the surfaces surrounding them, the mosaic generated from MI images of the central peak is draped over the SELENE orthorectified TC-DEM. Very high-resolution (~0.5-1.2 m/pixel) observation from Narrow Angle Camera (NAC) onboard the Lunar Reconnaissance Orbiter (LRO) (Robinson et al., 2010) have been utilized for identifying the observed features and associated structures on crater floor and central peak and and characterizing their mutual relations. False-colour composite (FCC) image is generated from the SELENE MI-VIS images after georeferencing and mosaicking them, by assigning red, green and blue colour to 950 nm, 900 nm and 750nm bands, respectively. The resultant image reveals the presence of compositionally different lithologies at the central peak and floor of crater Tycho.

In the fusion image (Figure 1) generated by draping the MI-VIS FCC image over SELENE orthorectified digital elevation model (DEM), two compositionally distinct geological units could be discriminated on the basis of their colour variations. The light brown colour in this image represent the impact melts present over the top of the central peak of crater Tycho, stalled

in its topographic depressions, flowing along the slopes, and spread over the crater floor. This melt bearing lithology has been inferred in earlier observations and their detailed study (Bray et al., 2010; Carter et al., 2012). The other major distinctive unit is in blue colour as could be observed alongwith the melt features. These exposures could be observed over the top of the ridges forming the central peak, their flanks and along the foothills. They are also observed along the cracks of impact melt sheet present on the floor of the crater Tycho (Figure 1). Similar lithological variability have been checked for and observed at central peak and floor of other contemporary craters of the Moon that includes Jackson, King and Copernicus (Figure 2). When analyzed from Moon Mineralogy Mapper (M^3) for mineral identification based on spectral characterization all were showing varied composition as detected from their acquired spectra (Figure 3). All are showing highland lithology with dominance of anorthosite along with variable amount of olivine, pyroxenes (both ortho and clino) and spinel. At Copernicus troctolite (olivine and plagioclase), Jackson and King anorthositic gabbro and norite and at Tycho the mafics with varying amount of plagioclase, pyroxenes, spinel, olivine are mainly anorthositic gabbro and troctolite. Some of these minerals were already reported from earlier observation using multiple datasets including Chandrayaan-1 M^3 and SELENE MI for these craters (e.g, Lemelin et al., 2015, Chauhan et al., 2012).

To further understand the nature of these mafic exposures as well as their stratigraphic relationship with the melts, these features were observed and analyzed using high-resolution NAC images for Tycho (Figure 4). The melts are characterized by their low albedo and smooth texture and appears to be forming thick to thin flows that drapes the underlying features. The bright features pertain to mafic lithology and have granular nature characterized by varied sized boulder clasts or remnants of solid broken melt crust. The mafics are also occurring in form of blocks of varying sizes ranging from few mm to tens of meters. Towards the top of the peak (figure 4a) they appear in form of thick massive lithic features partially embedded in the melt possibly part of thick melt sheet. At the flank of the central peak (Figure 4b) a large boulder clast ~45m could be seen partially covered by thin melt layer along with melt indurated small to medium-sized granular clasts drifted along by the flow. Along the flank slopes of the central peak, the mafics are in form of large to medium-sized boulders covered by overlying melt flows (Figure 4c & d). Towards the northeastern side over flank of a ridge (Figure 4e) with a distance from the top, fine granular flow occurs associated with fluid and turbulent melt flows. Their

movement is guided by melt free large obstacles that overlies the surface debris, both showing mafic nature. In-between the two flows the granular nature of mafics could be discerned characterized by its smooth texture. Downhill they are forming free debris flow poorly sorted by gravity and accompanying melt flow, showing scree and talus type depositional nature (Figure 4f). At the foothill they are scattered near the contact within the crater floor, in form fine to medium sized boulders. Along the flanks they are at times covered by melts flows and at times are exposed showing their granular nature. The boundary of individual flows had solidified and formed solid crust (Figure 4f). The pieces of solidified hard melt crust could be seen scattered along their margin. At the southeastern edge of the central peak a megablock having stratified nature about 200m long and 150m wide is present (Figure 5a) and similar characteristic bearing mafic features could be observed at other parts near the top of the central peak (Figure 5b).

At the crater floor the mafic exposures could be seen along the structural features such as fractures or cracks, where they are protruding in form of boulder clasts with or without intimately mixed melt (Figure 6a-c). Some of the cracks are wide and characterized by presence of numerous boulders with size ranging from ~25m to relatively medium and grading to even fine size along with smooth surfaced melt which later on cooled and developed cracks and now characterized by brittle crust and presence of regular fractures patterns along its edge. This poorly sorted clastic material appears to be partially squeezed out from the large cracks upward along with melt which is also sharing similar nature (Figure 6a and b). These megacracks are showing undulating and branching nature along their strike (Figure 6b). On the other hand clastic material still fills in small fissures (Figure 6c). The overall bright and rough positive topography present across the melt sheet observed at the crater floor could be reflecting their mafic nature that protrudes through the impact melt. At Jackson, King and Copernicus craters also the mafics in form of clastics are present at the flanks of central peak and filling the cracks over their floor.The only difference being melt/clast ratio that appears to be high at Copernicus and King than at Jackson and Tycho.

3. Results and Discussion

3.1 Nature of occurrence and Mineralogy

Present observations suggest that out of the two compositionally distinct lithologies marked at and near the central peak and crater floor of Tycho and the other contemporary craters, the one

occurring in light brown colour and forms more or less smooth and flow texture represent impact melt that occurs dominantly associated with impact craters. The other mafic bearing layer having variable composition occurs in blue colour are mostly in form of varied sized blocks. The poorly sorted nature of these blocks and their irregular shape with sharp edges as seen in the large boulders points towards the brecciated nature of these blocks. The partially or completely indurated melt clasts as well as without it and those present within the small cracks and megacracks, (Figure 4 and 5) could thus, be associated with polymict fragmental breccia clasts common in impact craters. Fragmental breccias clasts are formed by fracturing and faulting of the target rocks, during compression, and decompression phase of cratering (Dence, 1971; Grieve et al., 1977; Melosh, 1989) and occurs either in form of lithic breccias consisting of rock and mineral fragments or melt-fragment breccia better known as suevites containing both melt and mineral fragments. Their mafic nature could be attributed to the source of the clasts probably an underlying highland crust of anorthositic gabbro/norite composition that may also include shocked but unbrecciated anorthosites. Also, their association with brittle crustal fragments (e.g., Figure 4a) formed after solidification of melt layer suggests that some extent of partial recrystallization of the melt (Ogawa et al., 2011) would have contributed to their mafic signatures.

Parts of the Tycho's central peak as well as its crater floor, wherever present, it is observed that the breccias clasts are completely or partially covered by thin melt layer. It indicates that they are overlain by the melt and hence, emplaced prior to them. At other parts they are completely and integrally embedded within the melt suggesting that they are ejected in form of a combined melt-clast mass. The percentage of clasts varies as well as their grain size is also show variations. Near the top of the central peak and along its flanks and downhill they are mostly medium to fine-grained that could be due to gravity driven sliding and mass wasting associated with peak modification. The fine-grained clasts (ranging from 10mm-50mm) associated with highly fluid melt displaying multiple streamlines could be observed downslope over the flanks of the peak towards its west side (Figure 4c). They could be result of high-temperature combined melt-clast mass flow having high melt-volume from the top the peak leaving large blocks (e.g., Denevi, 2012). The light coloured melt-poor clasts indicate shock-crushed target rocks. The difference in size of the breccia fragments and tectonic setting suggest some reworking and redistribution associated with their emplacement.

3.2 Tectonic setting

At Tycho, the crater floor is mixture of melt and breccia clasts and most of the melt flows are overlying this brecciated crater floor. Major occurrence of the fragmented breccia material is observed along the fractures and cracks over the crater floor. The formation of these cracks have exposed the underlying lithology present in form of lithic clasts at some depths and distance from their wall. Similar fractures could be observed at Copernicus, King and Jackson crater floor where these mafic lithic brecciated clasts are exposed (Figure 2). Xiao et al. (2014) has mapped the distribution of the fractures on the floor of Tycho and Jackson and classified them based on their relative locations as internal and marginal, for those present near the centre and along its border between the crater wall and floor, respectively. These fractures as described forms network of polygonal or subparallel groups, mostly with widths consistent along their strikes and a few of them showed a trend of narrowing toward their ends. They were suggested to be extensional cracks formed by the cooling of the crust by thermal contraction or cooling-related subsidence that are generated at different times indicated by their cross cutting relation (Xiao et al. 2014). As observed their density is different in all of these craters under study and that may be due to different melt to clast ratio. As observed in high-resolution NAC images at Copernicus and King crater these fractures are less and relatively smooth (Figure 9b) in appearance in contrast with Jackson and Tycho where thay are widespread, more rough that occur in form of prominent parallel and polygonal features. The pattern of cooling fractures may differ due to presence of clasts in varying degree caused by anisotropic thermal stresses generated cooling (Denevi et al., 2012).

However, not all the fractures present at these crater floors are cooling cracks but some of them are perhaps the large fractures or megacracks (figure 6a and b). They are different in morphology and their dimensions are far larger than these cracks. Their width varies from more than ~200m and length from one to 10 kms. Here at Tycho the discrete clastic fragments are associated with some melts (Figure 7a-d) and most of the megacracks are associated with uplifted positive topography in form of doming (Figure 6b and 7d). As observed they are showing undulations in their width, bifurcation along their strike and branching nature. At Copernicus and King with melt dominant floor and less fractures, very few megacracks (Figure 9a & b) have been observed and that too relatively small in dimension; at Jackson a few megacracks could be seen with the most prominent one observed in the image (Figure 9c). At

Tycho more than six megacracks could be seen and are peculiar in appearance (Figure 6-8) not observed at any of the these crater floor. At Tycho most of them these megacracks are characterized by disturbance of the melt layer emplaced prior to it and marked by its minor displacement especially at their tip. However, at some intstance a minor melt layer could be observed that seems to have been placed at some later stage as revealed by its fresh nature (Figure 6b and 8a & b). Whenever this minor melt in form of patch is seen, it is characteristically showing a depression/pit over it (marked by arrow in Figure 6b and 8a & b). The peculiar mode of emplacement of the melt-breccia at these megacracks suggest them to have be emplaced tectonically at some later stage through some opening as the material seems oozing out and breaching their wall rocks. These megacracks or graben like features could therefore indicate opening tips of some underlying vertical or subverticle channel from which the clast-melt material have been expelled out and thus, characterizes breccia/melt dikes. They are common phenomenon associated with impact cratering and have been described from a number of terrestrial impact structures (e.g., at Vredefort, Koeberl et al., 1996; and at Sudbury, Stoffler et al., 1994). The breccias dikes as seen in the present observations at Tycho occur mainly around the central peak where they are thick and more or less parallel to them. Away from the centre they are relatively less common and oriented radially. Towards the north and north east side near to the crater rim of Tycho, a few dikes are recognized that are ~ 10 km long and oriented parallel to the rim.

3.3 Formation mechanism of dykes associated with cratering

Dykes are the most ubiquitous mesoscopic structural features that can form at both the early and late stages of evolution of an impact crater. Those formed in early stages are associated with transient cavity and central peak and are formed by injection of turbulent melt flow at the base of the melt sheet (e.g., Grant & Bite 1984; Murphy & Spray 2002, Tuchscherer & Spray 2002; Lightfoot & Farrow 2002). These catastrophic dykes are formed within few minutes after the impact (e.g., Grieve et al., 1977; Melosh, 1989; Hecht et al., 2008). Post-impact modification by flexural uplift of the crater floor during isostatic equilibration can also result in formation of dykes, that are formed on the order of tens to hundreds of thousands of years after the impact (Wichmann and Schultz 1993). These late stage dykes results in opening of fractures in the crater floor and are emplaced in a strain field characterized by radial and tangential dilation (Wichmann and Schultz 1993; Riller 2005; Hecht et al., 2008). Their thickness may vary between tens and

hundreds of meters and often characterized by intrusion of melt that may be derived from the evolving pre-existing impact melt sheet or endogenic melt (Wichmann and Schultz, 1993; Hecht et al., 2008). When visible these dykes appear in form of vein-fracture networks and are associated with breccia and melt or both. In the present context they may be termed as breccia dykes as at Tycho surface they appears mostly brecciated although melt is also present and could be observed in high-resolution LROC-NAC images (Figure 8). Their dimensions indicate them to be emplaced during post-impact events. Earth based studies also indicates that while impact melt dykes are few meters in width and length (e.g. at Manicouagan, Murtaugh, 1975; Dence, 1971; Phinney and Simonds; 1977; Floran et al., 1978) dykes associated with crater modifications may be tens to hundreds of meters wide and extend tens of kilometer into the surrounding rock (e.g., Sudbury dykes, Grant and Bite, 1984). The peculiar morphology with branching and bifurcating nature along strike is also characteristic of typical dykes. As observed they are spatially concentrated near the central peak in radial and concentric fashion.

3.4 Possible formation mechanism of oozed out material peculiar to Tycho settings

At Tycho some of these dykes are showing peculiar nature not observed at any other contemporary craters being studied. As mentioned earlier and could be observed in the (Figure 7) the clast material seems to have been forcefully placed on the both the sides of the dyke. Both the fragmented breccia clast and melt appears to have been placed episodically. Earlier studies based on Crater size-frequency distribution (CSFD) measurements at Tycho and other contemporary craters, suggested discrepancy in ages of its different units that have been attributed to various factors including different target properties, secondary cratering, different illumination conditions, late volcanism (Schultz and Spencer, 1979; van der Bogert et al., 2010; Ashley et al., 2011; Heisinger et al., 2012). Heisinger et al. (2012) concluded different target properties and/or self-secondaries would have resulted in that younger apparent absolute model ages for the impact melt pools which are geologically contemporaneous with the ejecta blanket. Kruger et al. (2012) have also noted the polygonal structures on the melt sheet of crater Tycho that showed less maturity then the rest of the melt sheet. One possibility in the given scenario is that the fractures/cracks that existed earlier as well as the pre-existing dykes in the stress zones were triggered by temperature fluctuations and the stresses induced may have resulted in generation of doming but in that case the material may not extrude out. The presence and

expelled nature of brecciated clasts could indicate their secondary descent at some later stage. The stress at the tip of dyke may have rip apart the rocks ahead allowing the material to squeeze out and offsetting the wall. Not only has the clast material, the melt also seems to ooze out which suggests small scale post-impact extrusions of melt material. The floor of the Tycho is flat (original impact crater shape have been altered) and lap up against both central peaks and terraces in the outer walls which suggest hydrostatic filling of a bowl-shaped depression and therefore indicate that it had undergone post-crater modification in terms of viscoelastic relaxation (Pike 1967; Melosh & Ivanov, 1999). Further anticlinal doming of the rock layers above interthrust wedges is result of thickening and uplift of the transient crater rim related dyke emplacement during late stage during isostatic readjustment. There is a possibility that the melt from underlying impact melt sheet or pool may have permeated into the crater basement via flexture induced surface fractures. These fissures or dykes loaded with clasts, which were than expelled out or forced upward with or without melt, therefore serve as conduits for the melt and clast or both agreeing with the nature of emplaced material.

The nature and mechanism of emplacement of the observed features could also be associated with seismic activity and there is a possibility that shock vibrations would have open the cracks. Recent reporting of fault scraps of late Copernican age and their association with shallow moonquakes (Watters et al., 2015; Kumar et al. 2016) further supports this. Another scenario could be possibility of reactivation of the dykes induced by some endogenetic activities as recently some young volcanic features in form of Irregular mare Patches (IMP) have been observed on the Moon (Braden et al., 2014). In that case high-thermal inertia as reported for Tycho supports that the target material is more consolidated and contains a large population of rocks (Elder et al., 2017) and the stresses induced by the accumulation of trapped gases may have resulted in generation of doming. It therefore indicate that the isostatically generated stresses would have resulted in the lithological variability reflected in form of exposed clasts at fractures and the emplaced material could be related with rejuvenation of dykes induced by viscoelastic relaxation either through melt emplacement or extrusion of endogenic material at some late stage. The present lithology and surface morphology is due to prolonged and involved alteration of crater floor that underwent isostatic readjustment and at Tycho the dykes were rejuvenated by combined effect of tectonic and endogenic or melt induced activity.

3.5 Implications for Crater modification Processes

Impact cratering is a dynamic and complex process. The emplacement style of impact melt and fragmental breccia and their relationship with rock deformation is one of the least understood process. It needs understanding and interpretation of the associated deformation features. The process is very rapid but not instantaneous, and operates in three stages namely, coupling, excavation and modification (Figure 10a and b). It causes topographic and lithological transformations and promotes intense structural and thermal modification of crust (e.g., Grieve 1987; Melosh 1989; Ivanov & Deutsch 1999) (Figure 10 b). The modification stage may oocur in form of gravitational adjustment, viscous relaxation and doming, cooling and solidification (Masaitis 2005) (Figure 10 c). Fracturing and associated brecciation is a common feature being distributed over the crater floor and could occurs in multiple stages with material derived from all layers of the target including uppermost and lowermost ones (Therriault & Grieve, 2002). The fractures associated with cratering vary in their length and are related inversely with the strain rate (Melosh 2005). The fractures generated in the early stage at high strain rates are short, closely spaced and often irregular to parallel whereas those generated during the modification stage may coalesces and become longer and are meters to kms long (Spray 1997; Melosh 2005; Kenkmann et al. 2014). So, while formation of cooling cracks, the small scale surface features that occurs due to slow cooling induced by thermal radiation (Howard & Wilshire, 1975; Xiao 2014), fractures that are generated in different stages of cratering, may vary in their length and can also result in formation of the dykes (Lambert 1981).

Impact melts and fragmental breccias, the byproducts of cratering are emplaced over the surface during its late-modification stage (Melosh, 1980). During excavation also a considerable amount of both fragmented breccia and melts are emplaced over the crater surface or injected via dykes (Kenkmann et al. 2014). An impact crater upon dissipation of the explosion, its physical conditions revert to those of the nonimpact surface environment; and lunar surface characterized by lack of erosional processes are capable of reducing the mass excess of substrata yield to the imposed stresses and deform viseoelastically (Pike, 1967). Geological data obtained from observation of terrestrial craters (Melosh and Ivanov, 1999) and numerical calculations for emplacement of Worthington offset dyke of Sudbury impact structure, Ontario (Hecht, et al., 2008) suggests that the viscous relaxation of a crater out of isostatic equilibrium occur at much longer time scale and can continue upto several thousand to about ten thousand years after the impact. The emplacement of late-stage dykes is related with formation of radial and concentric

fractures as a consequence of isostatic readjustment of crust below the crater. These dykes which are active for a long period of time due to crustal relaxations at later time can squeeze out partially either or both the loaded clasts or melt from the underneath melt pool (e.g Riller et al., 2010). Further the impact melts present beneath the floor that has been channelized later through the dykes cannot be distinguished from the lava flows as they are differentiated and therefore may show diversified lithology.

4. Conclusions

The two compositionally distinct lithologies differ in colour and specific appearance as identified and observed at and near the central peak of crater Tycho and other contemporary craters through high-resolution remote sensing suggest them to be related to melts and fragmental polymict breccias clasts. Their sratigraphic relation suggest that the emplacement of breccias either/both prior to the melts or along with it. While at some part of the central peak their occurrence above the melt could be related with tectonic stabilization of central peak. The granular nature of the clasts in form of boulder of varying sizes and their dispersive nature suggests them to be representatives of less shocked crystalline target bed rock exposed in form fragmental lithic breccias. At places they are showing stratified nature while at most they occur in form of melt-indurated breccias. Their occurrence, mode of emplacement and association with the melts as observed through high-resolution images are consistent with their derivation from the deep-seated target which are exposed by cratering during its late-modification stage. The observed mafic highland lithology resulted due to presence of clasts in form of fragmental breccias from the underlying crust.

At the crater floor these mafic fragments occur in association with structural features such as cooling cracks and breccia dikes. The morphologically different breccias dikes also differ in emplacement behavior of the associated breccias clasts from the more frequently occurring cooling cracks. Therefore, the exposed mafic lithology present in form of brecciated clasts distributed over the crater floor and occurring over central peak suggests different form and nature of their emplacement in association with the dominant melt lithology. Their occurrence in different tectonic environment is related to different stages of cratering. While at peaks their emplacement along with melt is related with melt generation at different phases and peak modification. At other they are representing unshocked to varying degree shocked underlying

exposures. At the floor of the central peak they are representing underlying material exposed through thermal cooling, while at other their emplacement in form of brecciated dyke suggests a tectonic activity during later or post modification stage related to viscoelastic relaxation of craters. Considering the young age of crater Tycho this model is consistent with relaxation through late-stage dyke emplacements that are also showing age difference and distinct compositional difference from the melt. We suggest that post cratering melt cooling, differentiation and later melt laden dykes together with extruded material would have resulted in the age difference. The isostatic adjustment as observed at Tycho when compared with other contemporary craters possibly could be due to some tectonic readjustment peculiar to Tycho which could be associated with its tectonic setting, thin crust and young age.

Acknowledgements:

We would like to acknowledge and thanks SELENE MI, LROC-NAC and Chandrayaan-1 Moon Mineralogy Mapper data teams for providing data through public access webportals. Datasets for this research are available in public domain and can be accessed from https://ode.rsl.wustl.edu/moon and https://darts.isas.jaxa.jp

References:

Ashley, J. W., DiCarlo, N., Enns, A. C., Hawke, B. R., Hiesinger, H., Robinson, M. S., Sato, H., Speyerer, E. J., van der Bogert, C. H., Wagner, R. V., Young, K. E., & the LROC Science Team. (2011). Geologic mapping of the King Crater region with an emphasis on melt pond anatomy: Evidence from subsurface drainage of the Moon. 42nd *Lunar and Planetary Science Conference,* abstract # 2437.

Boardman, J. W. *et. al*. (2011). Measuring moonlight: An overview of the spatial properties, lunar coverage, seleno location, and related level 1b products of the Moon Mineralogy Mapper. *Journal of Geophysical Research,* 116: E00G14.

Bray, V. J., Tornabene, L. L., Keszthelyi, L.P., McEwen, A. S., Hawke, B. R., Giguere, T. A., Kattenhorn, S. A., Garry, W. B., Rizk, B., Caudill, C. M., Gaddis, L. R., & Vander Bogert, C. H. (2010). New insight into lunar impact melt mobility from the LRO camera. *Geophysical Research Letters,* 37, L21202. doi.org/10.1029/2010GL044666.

Braden, S., Stopar, J., Robinson, M. *et al.* (2014) Evidence for basaltic volcanism on the Moon within the past 100 million years. *Nature Geoscience* **7,** 787–791 https://doi.org/10.1038/ngeo2252

Carter, L. M, Catherine, D. N. D., Bussey, B. J., Spudis, P. D., Patterson, G. W., Cahill, J. T., & Raney, R. K. (2012). Initial observations of lunar impact melts and ejecta flows with the Mini-RF radar. *Journal of Geophysical Research,* 117, E00H09. doi.org/10.1029/2011JE003911.

Chauhan, P, Kaur, P., Srivastava, N., Bhattacharya, S., Ajai, Kumar, K.A.S.K., & Goswami, J. N. (2012). Compositional and morphological analysis of high resolution remote sensing data over central peak of Tycho crater on the Moon: implications for understanding lunar interior. *Current Science,* 102, 7, 1041-1046.

Dence, M. R. (1971). Impact melts. *Journal of Geophysical Research*, 76, 5552-5565. doi.org/10.1029/JB076i023p05552.

Denevi, B. W., Koeber, S. D., Robinson, M. S., Garry, W. B., Hawke, B. R., Tran, T. N., Lawrence, S. J., Keszthelyi, L.P., Barnouin, O.S., Ernst, C. M., & Tornabene, L.L. (2012). Physical constraints on impact melt properties from Lunar Reconnaissance Orbiter Camera images. *Icarus*, 219, 2, 665-675.

Dhingra, D., Head, J.W., & Pieters, C.M. (2017). Geological mapping of impact melt deposits at lunar complex craters Jackson and Tycho: Morphologic and topographic diversity and relation to the cratering process. *Icarus*, 283, 268-281.

Elder, C.M., Hayne, P.O., Bandfield. J.L., Ghent, R.R., Williams, J. P., Donaldson Hanna, K.L., & Paige, D.A. (2017). Young lunar volcanic features: Thermophysical properties and formation. *Icarus*, 290, 224-237.

Floran, R.J., Grieve, .A.F., Phinney, W.C., Warner, J.L., Simomds, C., Blanchard, D.P. & Dence, M.R. (1978). Manicouagan impact melt sheet, Quebec, 1, stratigraphy, petrology and chemistry. *Journal of Geophysical Research*, 83, 2737-2759.

Grant, R. W., & Bite, A. (1984). The Sudbury Quartz Diorite Offset Dikes. In: *The geology and ore deposits of the Sudbury structure*, E. G., Pye, A.J. Naldrett and P.E. Giblin (Eds.) Special Publication. Toronto: Ontario Geological Survey, 275-300.

Grieve R. A. F., Reny G., Gurov E. P., & Ryabenko V. A. (1987). The melt rocks of the Boltysh impact crater, Ukraine, USSR. *Contributions to Mineralogy and Petrology*, 96, 56-62.

500 Grieve, R. A. F., Dence, M. R., & Robinson, P.B. (1977). Cratering processes: As interpreted
501 from the occurrence of impact melts. In: *Impact and Explosion Cratering*, D. J. Roddy, R. O.
502 Pepin and R. B. Merrill (Eds.), Pergamon Press, NY, 791-814.
503 Haruyama, J., Matsunaga, T., Ohtake, M., Morota, T., Honda, C., Yokota, Y., Torii, M., Ogawa,
504 Y., & LISM Working Group (2008). Global lunarsurface mapping experiment using the
505 Lunar Imager/Spectrometer on SELENE. *Earth Planets and Space*, 60, 243-256.
506 Hawke, B.R., & Head, J.W. (1977). Impact melt on lunar crater rims. In: *Impact and Explosion*
507 *Cratering.* D. J. Roddy, R.O. Pepin and R.B. Merrill (Eds.). Pergamon Press, NY, pp. 815-
508 841.
509 Hawke, B. R., Lucey, P. G. & Bell, J. F. (1986). Spectral reflectance studies of Tycho crater:
510 preliminary results. *Proc. 17th Lunar and Planetary Science Conference*, 999-1000.
511 Hawke, B.R., & Bell, J. F. (1981). Remote sensing studies of lunar dark-halo impact craters:
512 Preliminary results and implications for early volcanism. *Proc. 12th Lunar and Planetary*
513 *Science Conference*, 665-678.
514 Hecht, L., Wittek, A., Riller, U., Mohr, T., Schmitt, R.T., & Grieve. R.A.F. (2008).
515 Differentiation and emplacement of the Worthington Offset Dike of the Sudbury impact
516 structure, Ontario. *Meteoritics & Planetary Science*, 43, 1659-1679.
517 Hiesinger, H., van der Bogert, C. H., Pasckert, J. H., Funcke, L., Giacomini, L., Ostrach, L. R., &
518 Robinson, M. S. (2012). How old are young lunar craters ? *Journal of Geophysical*
519 *Research*, 117, E00H10, doi:10.1029/2011JE003935.
520 Heisinger, H., & Head, J.W. III (2006). New views of lunar geosciences: an introduction and
521 overview. *Reviews in Mineralogy and Geochem*istry, 60, 1-81.
522 Hiesinger, H., Vander Bogert, C. H., Robinson, M. S., Klemm, K., & Reiss, D. (2010). New
523 crater size frequency distribution measurements for Tycho crater based on Lunar
524 Reconnaissance Orbiter camera analysis. *41st Lunar and Planetary Science Conference*,
525 abstract # 2287.
526 Howard, K. A., & Wilshire, H. G. (1975). Flows of impact melt at lunar craters. *Journal of*
527 *Research of U.S. Geological Survey*, 3, 2, 237-251.
528 Ivanov, B.A., & Deutsch, A. (1999). Sudbury impact event: Cratering mechanics and thermal
529 history. In: *Large meteorite impacts and planetary evolution.* B.O. Dressler and V. L.
530 Sharpton (Eds.) Geological Society of America, Special Paper 339, 389-397.

Kato, M., Sasaki, S., Tanaka, K., Iijima, Y., & Takizawa, Y. (2008). The Japanese lunar mission SELENE: Science goals and present status. *Advances in Space Research*, 42, 294-300.

Kaur, P., Chauhan, P., Bhattacharya S., Ajai, & Kumar, A.S.K. (2012). Compositional diversity at Tycho crater: Mg-spinel exposures detected from Moon mineralogy mapper (M^3) data. *43rd Lunar and Planetary Science Conference*, abstract # 1434.

Kenkmann, T., Collins, G.S. & Wünnemann, K. (2012) The modification stage of crater formation. In: *Impact Cratering: Processes and Products. G.R.* Osinski and E. Pierazzo (Eds.),. John Wiley & Sons, Chichester, pp. 60-75.

Kenkmann, T., Poelchau, M.H., & Wulf, G. (2014). Structural geology of impact craters. *Journal of Structural Geology*, 62, 156e182.

Koeberl C., Reimold, W. U., & Shirey, S. B. (1996). Re-Os isotope study of the Vredefort granophyre: Clues to the origin of the Vredefort structure, South Africa. *Geology*, 24, 913-916.

Kruger, T., Vander Bogert, C.H., & Hiesinger, H. (2012). Distribution and model ages of impact melt pools at the lunar crater Tycho. *Europian Planetary Science Congress*, abstract # 7, 842-1.

Lambert, P. (1981). Breccia dikes—Geological constraints on the formation of complex craters. In: *Multi-ring basins: Formation and evolution.* P.H. Schultz and R.B. Merrill (Eds.), Pergamon Press: NY, 59-78.

Lemelin, M., Lucey, P. G., Song, E. & Taylor, G. J. (2015). Lunar central peak mineralogy and iron content using the Kaguya Multiband Imager: Reassessment of the compositional structure of the lunar crust. *Journal of Geophysical Research Planets*, 120, 869-887, doi:10.1002/2014JE004778.

Lightfoot, P. C., & Farrow, C. E. G. (2002). Geology, geochemistry, and mineralogy of the Worthington offset dike: A genetic model for offset dike mineralization in the Sudbury Igneous Complex. *Economic Geology*, 97, 1419-1446.

Masaitis, V.L. (2005). Morphological, structural and lithological records of terrestrial impacts: an overview. *Australian Journal of Earth Sciences*, 52, 509-528.

Melosh, H.J. (2005). The mechanics of pseudotachylite formation in impact events. In: *Impact Tectonics* H. Henkel and C. Koeberl (Eds.). Springer, Berlin, 55-80.

561 Melosh, H. J., & Ivanov, B. A. (1999). Impact crater collapse. *Annual Review of Earth &*
562 *Planetary Sciences,* 27, 385-415.
563 Melosh, H.J. (1980). Cratering Mechanics-Observational, Experimental, and Theoretical. *Annual*
564 *Review of Earth & Planetary Sciences,* 8, 626p.
565 Melosh, H.J. (1989). Impact Cratering: A Geologic Process. Oxford Univ. Press, New York.
566 *American Mineralogist,* 55, 1608-1632.
567 Murphy, A. J., & Spray, J. G. (2002). Geology, mineralization, and emplacement of the Whistle-
568 Parkin offset dike, Sudbury. *Economic Geology*, 97, 1399-1418.
569 Murtagh, J. (1975). Geology of the Manicouagan crypto-explosion structure. Ph.D. Thesis, The
570 Ohio State University.
571 Ogawa, Y., et al. (2011). The widespread occurrence of high-calcium pyroxene in bright-ray
572 craters on the Moon and implications for lunar-crust composition, *Geophysical Research*
573 *Letters,* 38, L17202.
574 Ohtake et al. (2009). The global distribution of pure anorthosite on the Moon. *Nature.*
575 461(7261):236-40. doi: 10.1038/nature08317.
576 Phinney, W. C., & Simonds, C. H. (1977). Dynamical implications of the petrology and
577 distribution of impact melt rocks. In: *Impact and Explosion Cratering,* D. J. Roddy, R. O.
578 Pepin and R. B. Merrill (Eds.), Pergamon Press, NY, 771-790.
579 Pike, R. J. (1967). Schroeter's Rule and the Modification of Lunar Crater Impact Morphology.
580 *Journal of Geophysical Research,* 72, 8, 2099-2106.
581 Pike, R. J. (1976). Crater dimensions from Apollo data and supplemental sources. *The Moon,*
582 12463-12477.
583 Riller, U. (2005). Structural characteristics of the Sudbury impact structure, Canada: Impact-
584 induced versus orogenic deformation-A review. *Meteoritics & Planetary Science,* 40,
585 11,1723-1740.
586 Riller U., Lieger D., Gibson R. L., Grieve R. A. F., & Stöffler, D. (2010). Origin of large-
587 volume pseudotachylite in terrestrial impact structures. *Geology,* 38, 619-622.
588 Robinson, M.S., Brylow, S.M., Tschimmel, M., Humm, D., Lawrence, S.J., Thomas, P.C.,
589 Denevi, B.W., Bowman-Cisneros, E., Zerr, J., Ravine, M.A., Caplinger, M.A., Ghaemi, F.T.,
590 Schaffner, J.A., Malin, M.C., Mahanti, P., Bartels, A., Anderson, J., Tran, T.N., Eliason,

E.M., McEwen, A.S., Turtle, E., Jolliff, B.L., & Hiesinger, H. (2010). Lunar Reconnaissance Orbiter Camera (LROC) instrument overview. *Space Science Reviews,* 150, 81-124.

Schultz, P. H., & J. Spencer (1979). Effects of substrate strength on crater statistics: Implications for surface ages and gravity scaling. *Lunar and Planetary Science Conference,* 10th, 1081-1083.

Kumar, P. S. et al. (2016), Recent shallow moonquake and impact-triggered boulder falls on the Moon: New insights from the Schrödinger basin. *Journal of Geophysical Research*, 121, 147-179, doi:10.1002/2015JE004850.

Spray, J.G. (1997). Superfaults. *Geology*, 25, 579-582

Stöffler, D., & Ryder, G. (2001). Stratigraphy and isotope ages of lunar geologic units: Chronology and standard for the inner solar system. *Space Science Reviews,* 96, 9-54.

Stöffler, D., Deutsch, A., Avermann, M., Bischoff, L., Brockmeyer, P., Buhl D., Lakomy, R. & Müller-Mohr V. (1994). The formation of the Sudbury structure, Canada, Toward a unified impact model. In: *Large meteorite impacts and planetary evolution II*, Dressler, B. O. & Sharpton, V.L. (Eds.), GSA Special Paper 339. Boulder: *Geolological Society of America,* 303-318.

Stöffler, D., Ryder, G., Ivanov, B.A., Artemieva, N.A., Cintala, M.J., & Grieve, R.A.F. (2006). Cratering History and Lunar Chronology, *Reviews in Mineralogy and Geochemistry*. 60, 519-596.

Therriault, A. M., & Grieve R.A.F. (2002). The recognition of terrestrial impact structures**.** *Bulletin of the Czech Geological Survey*, 77, 4, 253-263.

Tuchscherer, M. G., & Spray, J. G. (2002). Geology, mineralization, and emplacement of the Foy Offset Dike, Sudbury impact structure. *Economic Geology*, 97,1377-1397.

van der Bogert, C. H., Hiesinger, H., McEwen, A. S., Dundas, C., Bray, V., Robinson, M. S., Plescia, J. B., Reiss, D., Klemm, K. & the LROC Team (2010). Discrepancies between crater size-frequency distributions on ejecta and impact melt pools at lunar craters: An effect of differing target properties? *41st Lunar and Planetary Science Conference,* abstract # 2165.

Watters, T.R., Robinson, M.S., Collins, G.C., Banks, M.E., Daud, K., Williams, N.R., & Selvans, M.M. (2015). Global thrust faulting on the Moon and the influence of tidal stresses. *Geology*, 43, 851-854. doi:https://doi.org/10.1130/G37120.1.

Wichmann, R. W. & Schulz, P. H. (1993). Floor-fractured crater models of the Sudbury structure, Canada: Implications for initial crater size and crater modification. *Meteoritics & Planetary Science*, 28, 222-231. doi.org/10.1111/j.1945-5100.1993.tb00760.x

Xiao, Z., Zeng, Z., Li., Z., Blair, D. M., & Xiao, L. (2014). Cooling fractures in impact melt deposits on the Moon and Mercury: Implications for cooling solely by thermal radiation. *Journal of Geophysical Research: Planet*, 119, E004560. doi:10.1002/2013JE004560

Figures description:

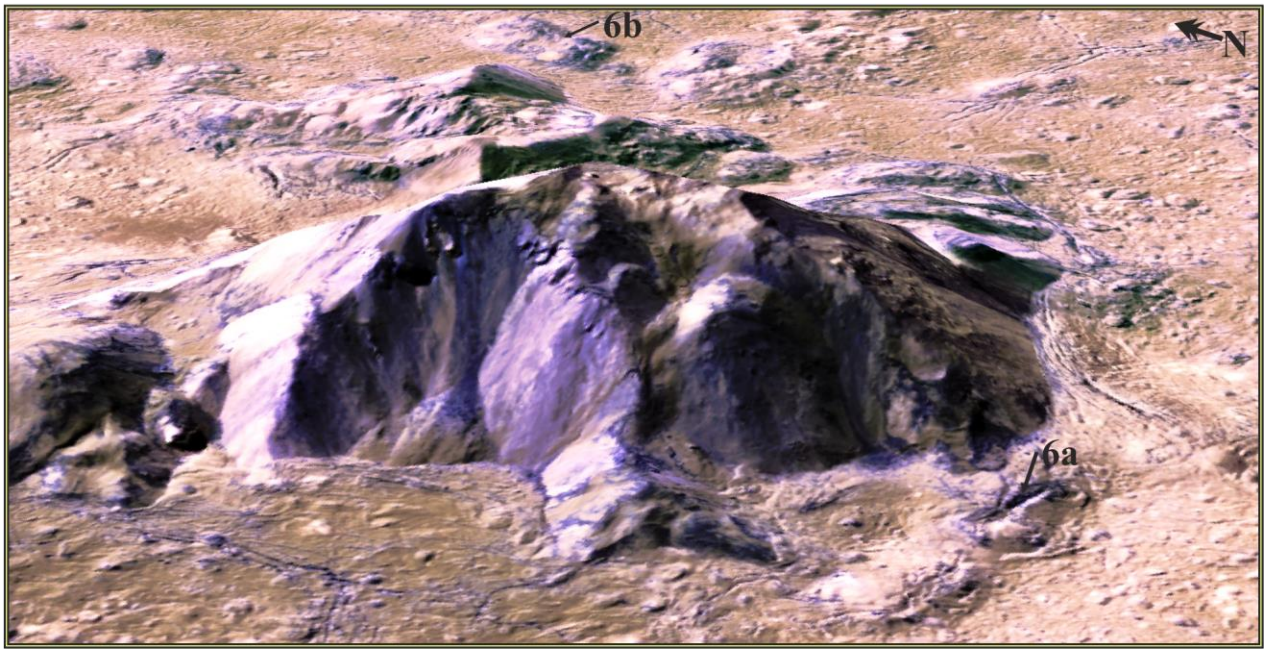

Figure 1: False colour composite (FCC) (R=950nm, G=900nm, B=750nm) of SELENE MI-VIS image draped over DEM for Tycho with vertical exaggeration of six showing variation in lithology from the colour difference. Two compositionally distinct lithologies are characterized by brown and dark blue colour.

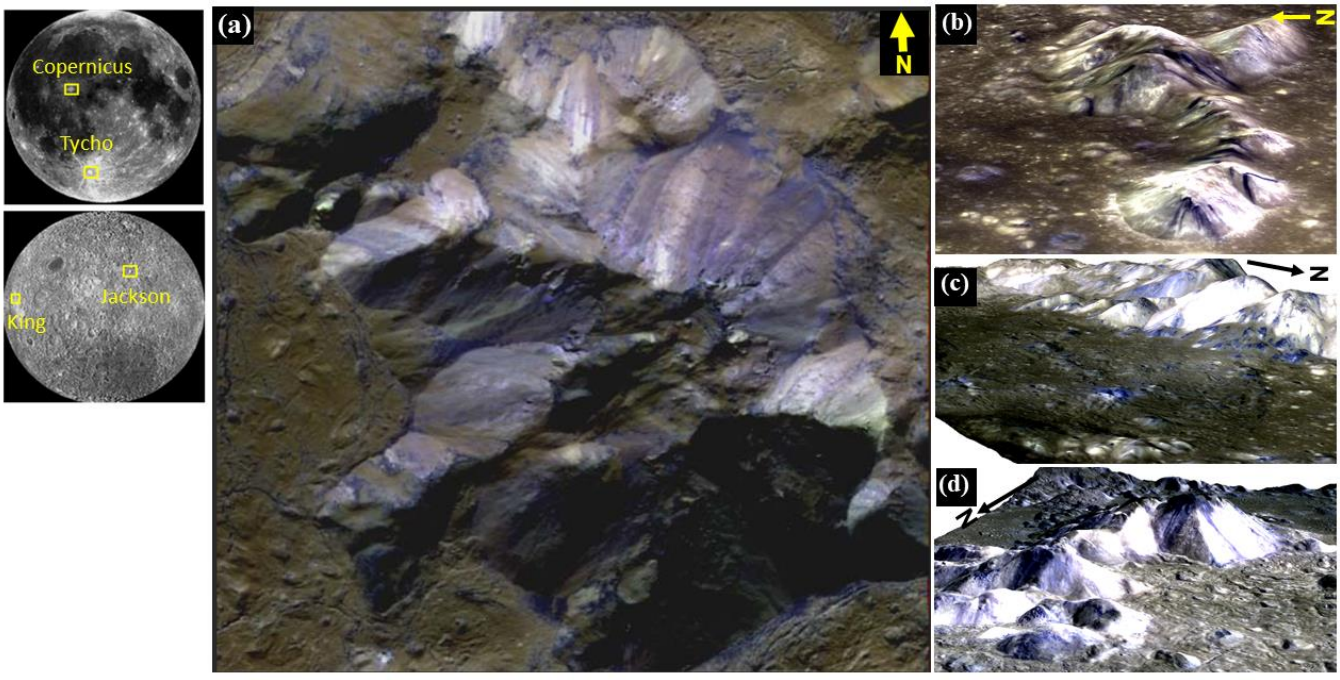

Figure 2: Location of four contemporary craters selected for the present study on the near and far side of lunar globe. False colour composite (FCC) (R=950nm, G=900nm, B=750nm) of

SELENE MI-VIS image draped over DEM with vertical exaggeration of seven, for (a) Tycho's central peak (upright view) showing variation in lithology from the colour difference; also observed at and near central peaks of (b) Copernicus (c) King and (d) Jackson crater.

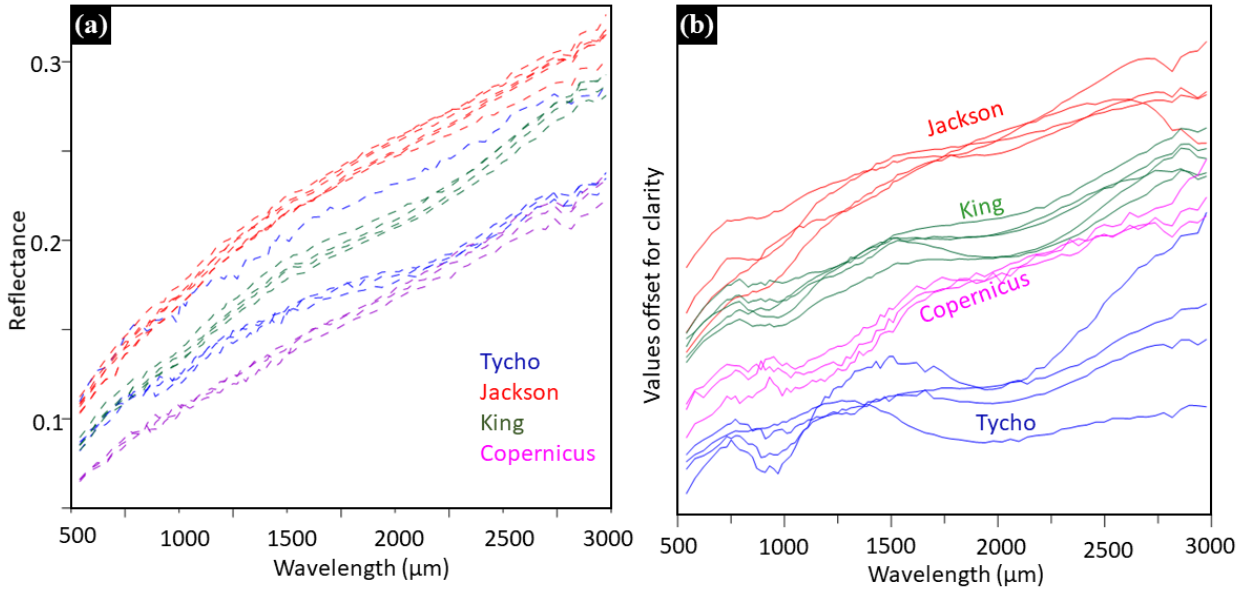

Figure 3: Chandrayaan-1 M^3 derived spectra of the two lithological units (a) melt and (b) fragmented breccia clasts as observed in figures 1 and 2 in brown and blue colour, respectively for the floor and central peak of crater Tycho, Jackson, King and Copernicus.

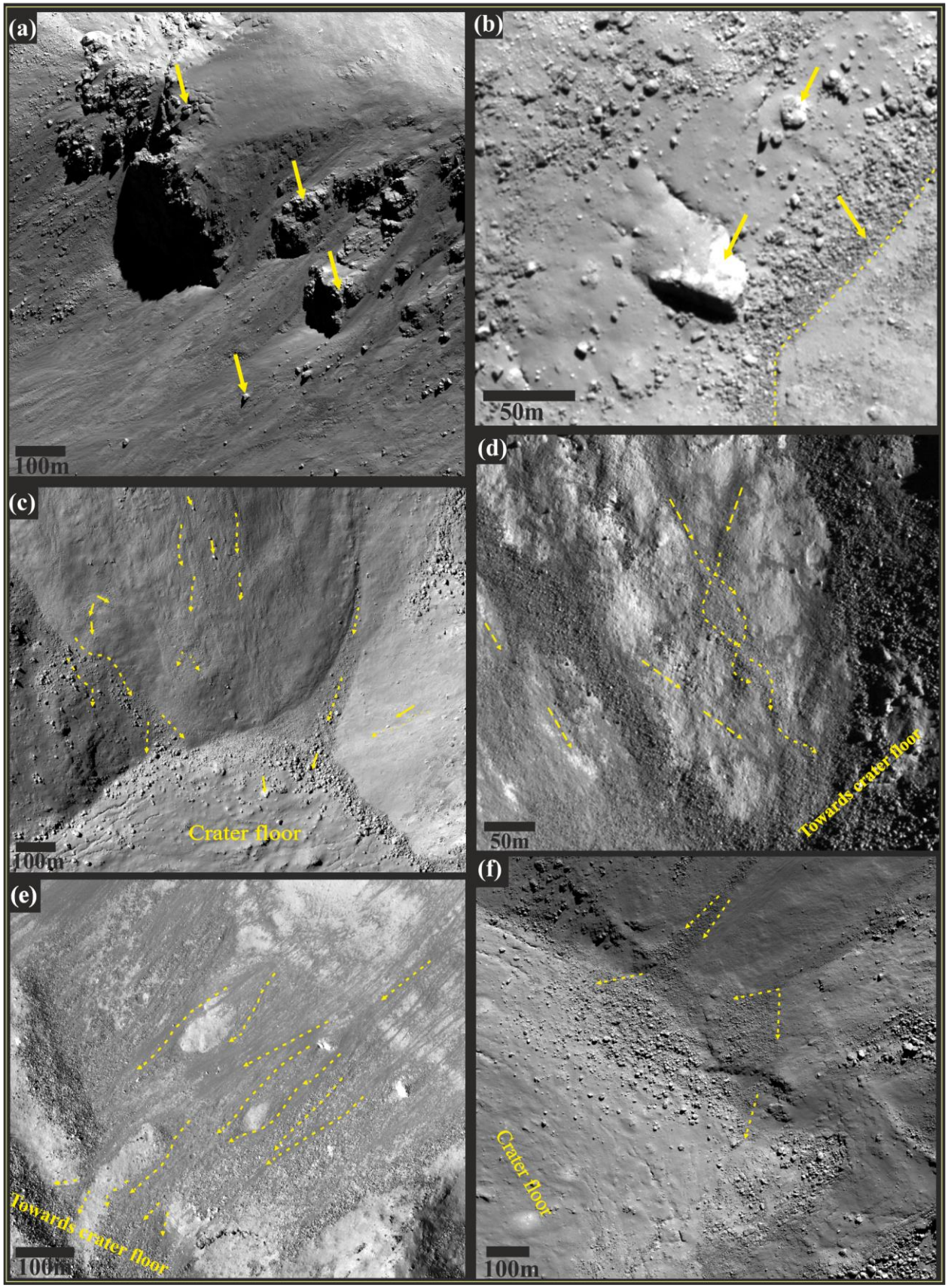
(a)
100m
(b)
50m
(c)
Crater floor
100m
(d)
Towards crater floor
50m
(e)
Towards crater floor
100m
(f)
Crater floor
100m

662

Figure 4: Subsets of LROC-NAC images for Tycho crater at high-resolution (1.5m/px) showing (a) the top the the central peak partially covered with thick melt flows and embedded massive and intact underlying lithic unit (b) Varying sized clasts partially covered or embedded in the melt and clustered granular clasts inbetween melt flows (c) Melt layer over the slope with overlying thin viscous fine granules embedded flow and boulders clustered near the foothill by debris slump or creep by melt flow, arrow indicates the boulder completely covered by melt, other partially covered, and bright exposed boulder; stippled arrows indicate their direction of movement. (d) Clast rich granular turbulent melt flow, smooth clast poor flow accompanied by fine debris flow (e) Fine turbulent flows overlying the granular surface debris and with their movement guided by large obstacles. Smooth and thin flows along the slopes with movement guided by underlying surface converging near the foothill (f) Rough and viscous flows characteriszed by dark albedo, cracks, brecciated hard crust; with relatively bright smooth and thin flows. Debris flow converging near the foothill guided and covered by impact melts. Downslope is towards the left of the image. flows of dry, fine-grained granular debris.

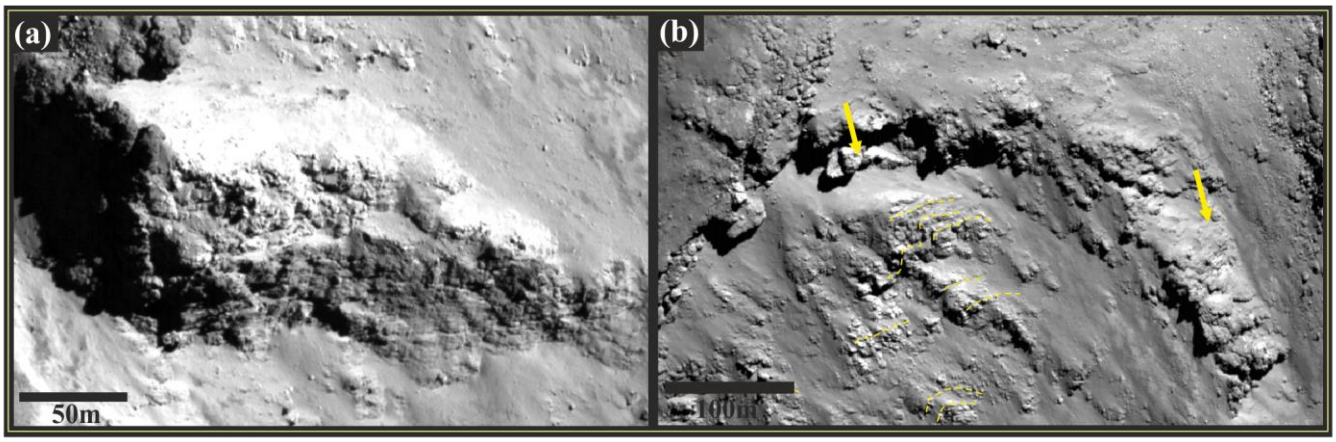

Figure 5: (a) Melt flows guided by nature of underlying beds of mafics, arrow indicating the partially exposed strata's while the stippled lines indicates their nature of deposition (b) Exposed megablock present over the southeast edge of central peak showing stratified nature.

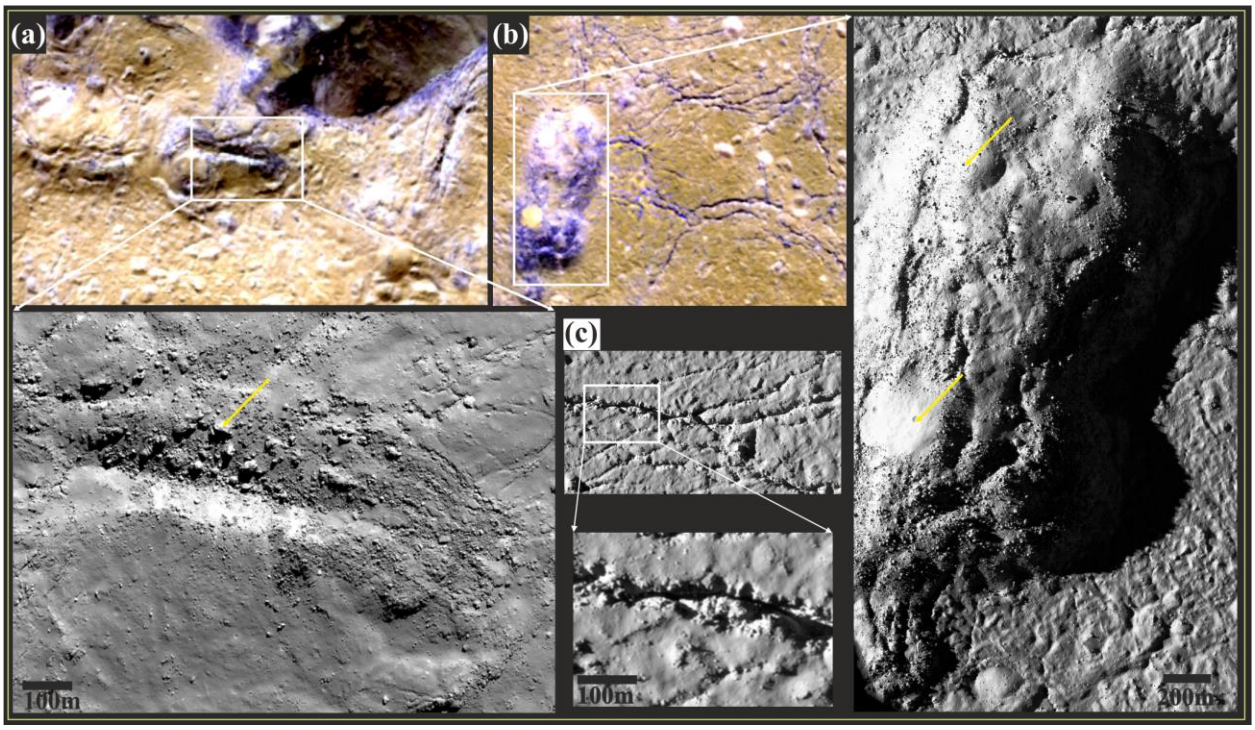

Figure 6: (a) Clastic material exposed at large fracture, boulders scattered in the melt near this megacrack at the crater floor (b) Similar exposure about 16km north of central peak within the floor showing melt indurated clasts within fractures and fresh melt exposure (c) Minor polygonal cracks present over the floor with relatively less deformed wall boundary and their parallel nature

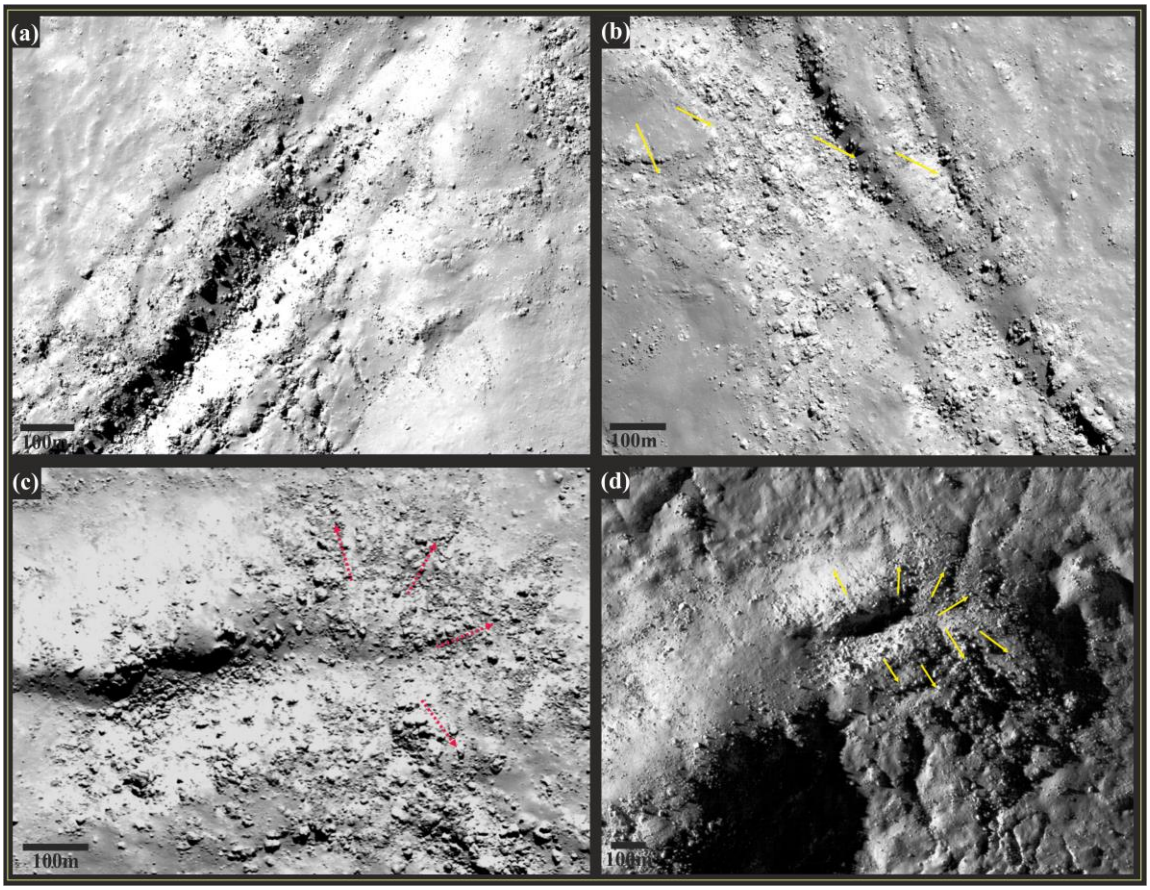

Figure 7: Subsets of LROC-NAC showing the brecciated dikes as observed at the floor of crater Tycho towards (a) west (b) southwest (c) and (d) north west side showing varied morphology and forceful emplacement behavior of breccias clasts and melts.

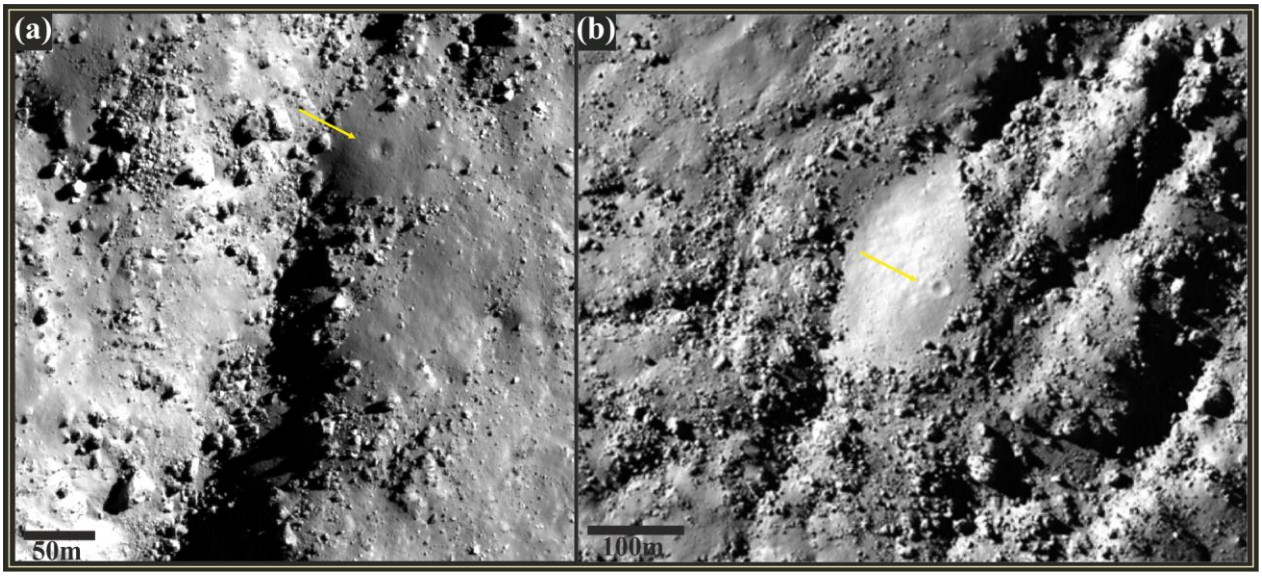

Figure 8: Subsets of LROC-NAC showing close-up view of brecciated dykes at Tycho crater floor with associated patch of impact melt with a small depression over it as indicated.

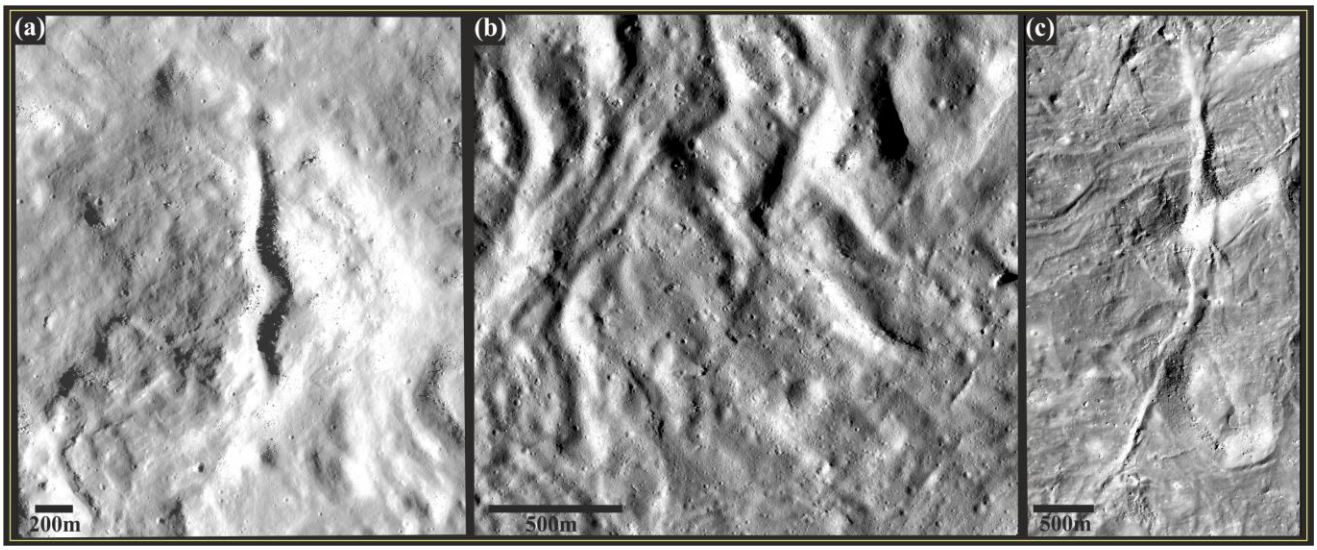

Figure 9: LROC-NAC subsets from the crater floor showing distribution of (a) Small dyke present at the towards the east of Copernicus central peak (b) View of smooth but wrinkeled surface of King crater (c) Large dyke present at the towards the north of Jackson crater**.**

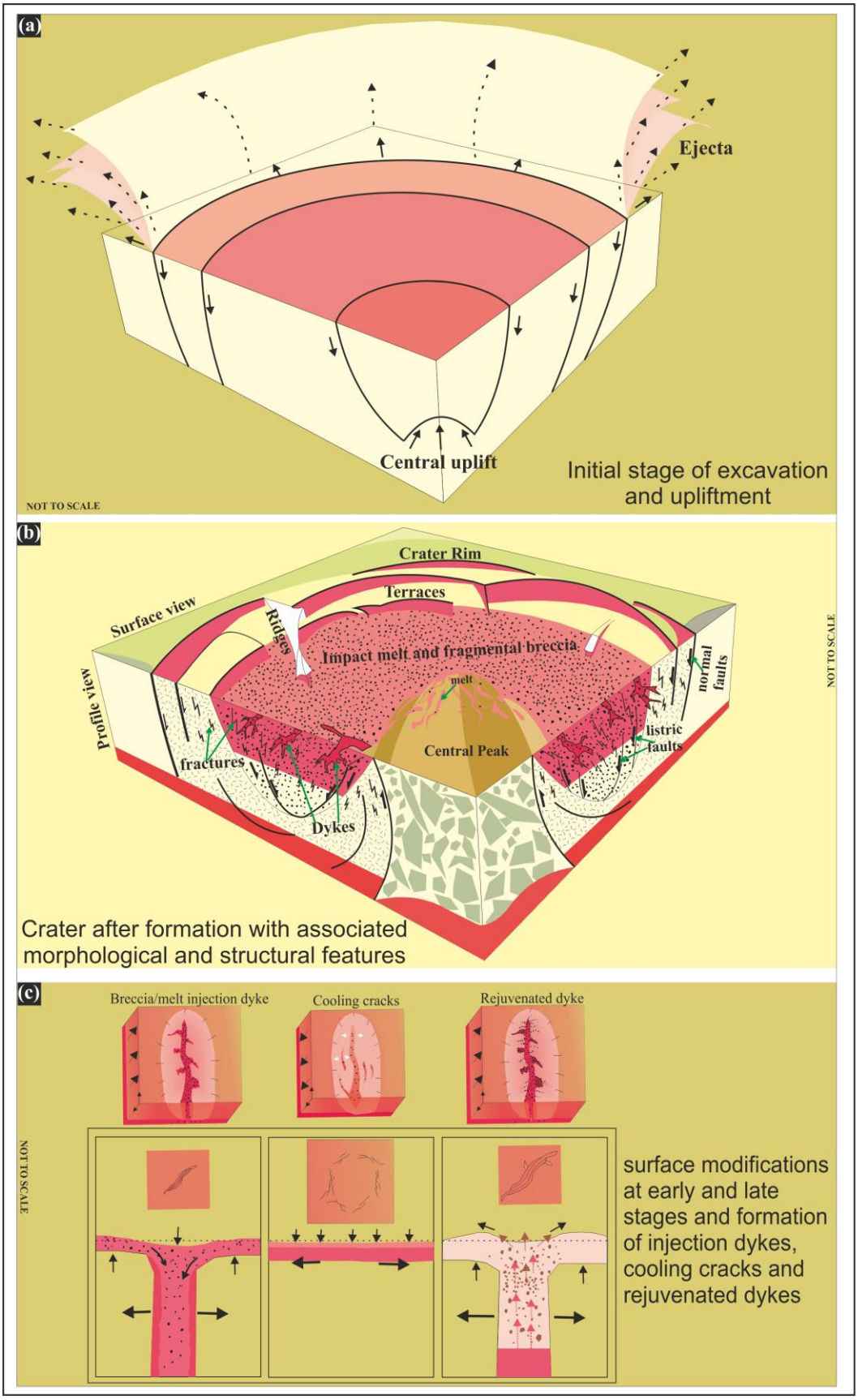
(a)
Ejecta
Central uplift
NOT TO SCALE
Initial stage of excavation and upliftment
(b)
Crater Rim
Terraces
Surface view
Ridges
Impact melt and fragmental breccia
melt
Profile view
normal faults
listric faults
Central Peak
fractures
Dykes
NOT TO SCALE
Crater after formation with associated morphological and structural features
(c)
Breccia/melt injection dyke
Cooling cracks
Rejuvenated dyke
NOT TO SCALE
surface modifications at early and late stages and formation of injection dykes, cooling cracks and rejuvenated dykes

702

Figure 10: Schematic block diagrams and their profiles showing the various stages, associated processes, characteristics structures and surface features generated during complex crater formation (a) Initial stages of complex cratering process with forces acting at different points during excavation and upliftment process (b) Complex crater after its formation showing distribution of various structural and morphological features (Modified after Kenkmann et al., 2012) (c) Formation of small breccia/melt dykes during intial excavation stages due to injection of either/both brecciated and melt material; formation of cooling cracks due to shrinking of the crust induced by thermal cooling and mega dykes generated during late stages of crustal modification accompanied by squeezing out of underneath material.